SUSTAINED ANTIBACTERIAL EFFECT OF LEVOFLOXACIN DRUG IN A POLYMER MATRIX BY HYBRIDIZATION WITH A LAYERED DOUBLE HYDROXIDE

Su-Joung Ko, Jin-Song Jung, Gyeong-Hyeon Gwak, Hyoung-Jun Kim, Fabrice Salles, Jae-Min Oh

SUSTAINED ANTIBACTERIAL EFFECT OF LEVOFLOXACIN DRUG IN POLYMER MATRIX BY HYBRIDIZATION WITH LAYERED DOUBLE HYDROXIDE

Su-Joung Ko[1], Jin-Song Jung[2], Gyeong-Hyeon Gwak[3], Hyoung-Jun Kim[4,*], Fabrice Salles[5,*], Jae-Min Oh[1,*]

[1] Department of Energy and Materials Engineering, Dongguk University-Seoul, Seoul 04620, Korea

[2] Department of Chemistry and Medical Chemistry, College of Science and Technology, Yonsei University, Wonju 26493, Republic of Korea

[3] Beamline Research Division, Pohang Accelerator Laboratory, Pohang University of Science and Technology, Pohang, Gyeongsangbukdo 37673, Republic of Korea

[4] Research Institute, National Cancer Center, 323 Ilsan-ro, Goyang, Gyeonggi 10408, Republic of Korea.

[5] ICGM, Univ. Montpellier, CNRS, ENSCM, Montpellier, France

Correspondence

Prof. Jae-Min Oh: jaemin.oh@dongguk.edu

Department of Energy and Materials Engineering, Dongguk University-Seoul

Tel: +82 2 2260 4977

Dr. Hyoung-Jun Kim: hjkim@ncc.re.kr

F. Salles fabrice.salles@umontpellier.fr

ABSTRACT

Immobilization of antimicrobial drug is one of the fascinating approach to expand the application of antibacterial property to consumer product. In order to stabilize antimicrobial agent, levofloxacin (LVX), into polymer substrate for sustained antibacterial activity, the drug molecules were immobilized in layered double hydroxide (LDH) and embedded in polyurethane substrate. As prepared MgAl-LDH was calcined at 400°C and reconstructed with LVX for intercalation. The X-ray diffraction patterns and cross-sectional transmission electron microscopy images showed lattice expansion along the crystallographic c-axis upon LVX intercalation, suggesting the successful loading of the drug. Fourier-transformed infrared spectra revealed that intact structure of LVX was well preserved between LDH layers. Elemental analysis indicated that the loading capacity of LVX in the hybrid was 41.7%. Bacterial colony forming inhibitory assay of exhibited ~100% antibacterial activity for both LVX alone and LVX-LDH hybrid (LL) on *Bacillus subtilis*. To determine sustainability of antibacterial activity by the hybrid, either LVX alone or LL hybrid was loaded in polyurethane (PU) substrate of which antibacterial activity was evaluated before and after immersing in phosphate buffered saline for 3 days. The LVX composited PU showed dramatic decrease in antibacterial activity down to 0% after buffer treatment; however, LL composited PU still contained antibacterial activity (~34% of colony suppression) after phosphate buffered saline immersion.

Key word: Layered double hydroxide, Levofloxacin, Intercalation, Nanocomposite, Sustainability, Antibacterial activity

INTRODUCTION

Bacterial infection is one of the most critical problems in biomedical application field being remaining as a serious threat to human life (Hu et al., 2017). Studies have shown that bacteria attach on the surface of the material and grow to form biofilm with the extracellular matrix, which is one of the essential causes of material infection (Wang et al., 2016). Bacterial biofilms have several hundred times stronger antibiotic resistance than floating bacteria (Hoffman et al., 2005; Traba & Liang, 2015). Infection by biofilm is becoming a potential risk factor in biomedical products like catheter and implant, resulting in the critical threatening to patients (Garcez et al., 2007; Conlon et al., 2013). Therefore, it is required to develop a method to effectively introduce antibiotics to the biomedical devices to prevent potential infection.

Many researchers tried to load antibiotics in medical polymers for antibacterial activity. Olanoff groups have developed gentamicin loaded silicone rubber to reduce infection on prosthetic heart valve in dogs (Olanoff et al., 1979). Lucke et al., reported that gentamicin incorporated poly(D,L-lactide) (PDLLA) coating layer on titanium Kirschner wires significantly reduced infection in rat-implants (2003). However, antibiotic loaded polymeric matrix showed burst release of drug resulting in failure of long-term antibacterial activity (Ragel & Vallet–Regí, 2000; Hong et al., 2018)To control drug release from polymer matrix, various strategies have been applied. For example, antibiotic molecule was encapsulated by β-cyclodextrin and then grafted to polypropylene mesh for sustained efficacy for several days (Sanbhal et al., 2018). Antibiotic can be directly conjugated to polymer for sustained release of drug and prolonged efficacy (Zhang et al., 2019). Sandwiching drug moiety between plasma polymerized layers has been suggested an alternative to control release of drug from solid carrier (Vasilev et al., 2011). Immobilization of drugs in nanoparticle be applied for this purpose, exemplified by the composite between polymer and antimicrobial drug loaded nanoparticles (Pinto et al., 2011; Saha et al., 2014; Patel et al., 2016). In this strategy, nanomaterials utilized as support of antibiotic drug for immobilizing drug or delaying drug release (Pinto et al., 2011; Saha et al., 2014). As a support for antibacterial drug, many inorganic materials such as zeolite (Khodaverdi et al., 2016), hydroxyapatite (Geuli et al., 2017), silica gel (Latifi et al., 2017) and etc. are used. Among them, layered double hydroxide (LDH), one of the clay minerals, is fascinating candidate of drug support. It consists of positively charged metal hydroxide layers and interlayer anions, with general chemical formula as $M(II)_{1-x}M(III)_x(OH)_2(A^{n-})_{x/n}\cdot mH_2O$ (M(II): divalent metal cation, M(III): trivalent metal cation, A^{n-}: interlayer anion, $0.2 < x < 0.4$) (Cavani et al., 1991; Rives, 2001). In

terms of biomedical application, LDH has various advantages such as anion capacity, biocompatibility, controlled drug release and etc (Choy et al., 1999; Choy et al., 2000; Senapati et al., 2016). As LDH can incorporate and immobilize anionic antibacterial drugs in its gallery space, the drug-LDH loaded polymer composite would have sustained antibacterial activity through controlled release.

In this study, a composite polyurethane (PU, as biocompatible polymer substrate) and levofloxacin (LVX, as an antibiotic) intercalated LDH (as a support for antibiotic) was prepared in order to demonstrate prolonged antibacterial activity. LDH was first applied to encapsulate LVX and the hybrid was then composited with PU polymer. As LVX is a water soluble drug, simple coating or mixing would not guarantee its stabilized attachment on the substrate. As aforementioned, the encapsulation of LVX in LDH is considered not only enhance the attachment efficiency toward a substrate but also provide the surface of substrate with drug moiety in controlled manner. First, hybrid between LVX and LDH was synthesized by dehydration and rehydration route, i.e, reconstruction (Kim et al., 2016a). In order to investigate structure of LVX-LDH (LL) hybrid, X-ray diffraction patterns, Fourier-transform infrared spectra and scanning electron microscopy were carried out. Through quantitative chemical analyses, the chemical formula and LVX content of LL hybrid could be defined. From the cross-sectional TEM image and energy dispersive spectroscopy, it was confirmed that the interlayer distance and elemental distribution of LL hybrid. The antibacterial activity of LVX and LL hybrid was evaluated by bacterial colony forming inhibitory assay against Bacillus subtilis. The long-term antibacterial activity of both LVX-PU and LL-PU composite was compared after immersing both composites in physiological buffer solution for 3 days.

EXPERIEMNTAL

Material

Magnesium nitrate hexahydrate ($Mg(NO_3)_2 \cdot 6H_2O$), aluminum nitrate nonahydrate ($Al(NO_3)_2 \cdot 9H_2O$) were purchased from Sigma-Aldrich Co. LLC (St. Louis., Missouri, USA). Sodium hydroxide pellets (NaOH) and sodium bicarbonate ($NaHCO_3$) were obtained from Daejung Chemicals & Metals Co., Ltd. (Siheung, Korea). Levofloxacin ($C_{18}H_{20}FN_3O_4$) was acquired from Tokyo Chemical industry Co., Ltd. (Tokyo, Japan). N-Methyl-2-pyrrolidone (NMP, C_4H_9NO) was obtained from Junsei Chemical Co., Ltd. (Tokyo, Japan).

Polyurethane (PU) film was purchased from CY. International Co., Ltd. (Seoul, Korea). All reagents were utilized without further purification.

Synthesis of pristine LDH and levofloxacin intercalated LDH nanohybrid

The pristine MgAl-LDH was prepared by conventional coprecipitation and consecutive hydrothermal treatment (Kim et al., 2018). A mixed metal solution (0.3 mol/L $Mg(NO_3)_2{\cdot}6H_2O$ and 0.15 mol/L $Al(NO_3)_2{\cdot}9H_2O$) was titrated with an alkaline solution (0.9 mol/L NaOH and 0.675 mol/L $NaHCO_3$) until pH 9.5. The obtained slurry was transported to a teflon-lined autoclave bomb and then treated at 100 °C for 48 h. The resulting white suspension was centrifuged, thoroughly washed with deionized and lyophilized. The synthesized pristine LDH powder was placed in alumina boat and calcined under muffle furnace at 400 °C for 9 h with heating rate of 0.8 °C/min. The calcined LDH is designated as layered double oxide (LDO). In order to prepare levofloxacin (LVX) intercalated LDH hybrid (LL), powdered LVX was dispersed in deionized water (0.225 mol/L) and titrated with alkaline solution (0.1 mol/L NaOH) until pH reached ~10.0 for deprotonation. The LDO powder was added to the LVX solution with vigorously stirring under N_2 atmosphere for 10 days. The stoichiometry between Al in LDO and LVX was set 1.5. The product was collected by centrifugation (10,000 rpm, 5 min) and lyophilized.

Characterization of LL

The crystal structures of pristine LDH and LL hybrid were investigated by powder X-ray diffractometer (XRD) at the 8D XRS POSCO beamline using Cu K-alpha, Pohang Accelerator Laboratory (PAL), Korea. XRD patterns were measured in the range from 1°2θ to 30°2θ with the time step increment of 0.02° and scanning rate of 0.5 sec/step. The compositions of metallic element of LL hybrid were analyzed by inductively coupled plasma-optical emission spectrometer (ICP-OES; OPTIMA 7300DV, PerkinElmer, Waltham, Massachusetts, USA). The powdered sample was dissolved in hydrochloric acid which was evaporated on a hot plate. The remnant was diluted with 100 mL of deionized water and filtered with syringe filter (PTFE, 0.45 μm, 13 mm, ADVANTEC®, Toyo Roshi Kaisha, Ltd, Tokyo, Japan) for ICP measurement. The loading capacity of LVX in LL hybrid was quantified by CHNS elemental analysis (2400 Series II CHNS/O Analyzer, PerkinElmer, Waltham, Massachusetts, USA). The intact structure of LVX in LL hybrid was evaluated by Fourier transformed infrared (FT-IR; Spectrum one B.v5.0, Perkin Elmer, Waltham, Massachusetts, USA) spectroscopy. FT-IR spectra were obtained by conventional KBr pellet method in the range from 450 cm^{-1}

to 4000 cm^{-1}. The morphology and particle size of the prepared samples were confirmed by scanning electron microscopy (SEM) using a Quanta 250 FEG (FEI Company, Hillsboro, OR, USA). For the SEM measurement, the samples were dispersed in deionized water. Then the suspension was dropped on a silicon wafer and dried. The surface of the specimen was sputtered with Pt/Pd for 60 s, and the images were obtained using a 30 kV accelerated electron beam. The cross-sectional morphology and interlayer distance of LL hybrid were determined by Field Emission Transmission Electron Microscope (FE-TEM; Titan G2 ChemiSTEM Cs probe, FEI company, Hillsboro, OR, USA) operated at an accelerating voltage of 200 kV. Powdered sample was fixed in Eponate 12 resin and the slices of specimens for cross-sectional observation were prepared with Cryo Ultramicrotome (CUMT; PT PC Ultramicrotome & Photographic, Boeckeler Instruments, Inc, Tucson, Arizona, USA).

Preparation of LVX-PU and LL-PU composite

In order to determine the molecular distribution of LVX ions in the LDH interlayer space, Monte Carlo simulations were performed using a homemade code.

The initial step consists into determining the structure of LVX. It was built and optimized using density functional theory (DFT) calculations (with the code DMol[3]). Then the partial charges were evaluated. For that purpose, optimization was performed using GGA/PW91 functional combined with DNP basis set. Furthermore, all electrons were considered for the core treatment. The convergence parameters for energy, maximum force, and maximum force variation were 10^{-5} Ha, 0.02 Ha/Å, and 0.005 Å, respectively.

The structure of LDH was taken from the literature by modifying the chemical composition in order to be close to the experimental composition, while the simulated unit cell parameters were fixed to the ones obtained experimentally. For the LDH structure, partial charges were calculated using the electronegativity equalization method. The Lennard-Jones parameters were issued from universal force field (UFF). A multi-cell formed by 3×3×1 unit cells for LDH was used for Monte Carlo calculations, in agreement with a fixed cut-off value for Lennard-Jones contributions of 12.5 Å. The Lorentz-Berthelot combining rule were used to determine the Lennard-Jones parameters for the adsorbate/adsorbent. For long-range electrostatic interactions, the summation Ewald technique was applied.

The simulations were performed in order to minimize the system energy by introducing a fixed

number of ions in the structure. During these calculations, the motion of the ions included translation and rotation randomly considered during the equilibration steps. For that purpose, 2×10^7 Monte Carlo production steps following 2×10^7 equilibration steps were performed at 300 K to extract the maximum saturation in LVX (in agreement with the electrical neutrality of the solid and containing ions), distribution of interlayer ions as well as the snapshots illustrating the interaction between LVX and LDH layers and between 2 LVX.

Preparation of LVX-PU and LL-PU composite

In order to prepare LVX-PU and LL-PU composite, first, 1 g of PU film was cut into small pieces and were located in a vial. Then, 10 mL of NMP was added to vial and stirred at 60 °C for 4 h on hot plate to completely melt the PU film. Then, LVX or LL powder was added to the PU solution with equivalent LVX concentration of 5.0 mg/mL. The PU solution containing either LVX or LL powder was transferred to 50 mL beaker. The PU solution was dried at 60 °C on a hot plate for 3 days in a fume hood. Then, LVX-PU or LL-PU composite was separated from the beaker using tweezers.

Release study

Time-dependent release profiles of LVX from the LL hybrid was obtained as follows. Hybrid powder (10 mg) was dispersed in 50 mL of saline media (JW Pharmaceutical Co., Ltd., Seoul, Korea). Aliquots (1 mL) were collected at determined time points, and then centrifuged at 12,000 rpm for 10 min and filtered with a syringe filter. The amount of released LVX in the supernatant was quantified with visible light spectroscopy (Varioskan LUX multimode microplate reader, Thermo Fisher Scientific, Waltham, Massachusetts, USA) at wavelength of 330 nm. Experiments were performed in triplicate.

The time dependent release behavior of LVX was analyzed by various kinetic models including first-order equation (Eq. 1), Elovich equation (Eq. 2) and Power function (Eq. 3).

$$lnQ_t = lnQ_e - kt \quad (1)$$

Where k is first-order rate constant (h^{-1}).

$$Q_t = a + blnt \quad (2)$$

Where a is released quantity in the initial phase and b is release rate.

$$Q_t = \alpha t^{\beta} \quad (3)$$

Where α is constant related to the initial desorption rate and β is desorption rate coefficient.

Q_t is the released amount at time t (min) and Q_e is the released amount at equilibrium form all models.

Evaluation of antibacterial activity of LVX and LL hybrid

The antibacterial activity of LVX and LL hybrid was evaluated against gram-positive bacterium, *Bacillus subtilis* (*B. Sub*) utilizing colony forming inhibitory assay. The 0.5 mL of LVX solution or LL hybrid suspension with equivalent LVX concentration of 1.0 ppm was mixed with 1.5 mL of the suspensions of *B. Sub* (2.0×10^6 bacteria) and inoculated in incubator at 37 °C for 8 h. Then, the incubated bacteria suspension was collected, diluted to 1.0×10^3 bacteria/mL and spread on culture agar plates. The agar plates containing bacteria were incubated at 37 °C for 12 h. The number of colonies was counted utilizing digital camera and a colony counting program (Image Processing and Analysis in Java; ImageJ) to calculate antibacterial activity. All the antibacterial tests were run in triplicate.

Antibacterial activity of LVX-PU and LL-PU composite

The antibacterial activity of LVX- and LL-PU composite was evaluated against B. Sub utilizing colony forming inhibitory assay. Each composite was located in a 45 mL of conical tube and then sterilized with ultraviolet irradiation for 30 min. The suspensions of B. Sub (9.9×10^5 bacteria) was added to the tube containing the composite and inoculated at 37 °C for 3 days. The conical tube without composite was utilized as a control group. Then the incubated bacteria suspension was collected, diluted to 1.0×10^3 bacteria/mL and spread on culture agar plates. The agar plates containing bacteria were incubated at 37 °C for 12 h. The number of colonies was counted utilizing digital camera and a colony counting program (Image Processing and Analysis in Java; ImageJ) to calculate antibacterial activity. All the antibacterial tests were run in triplicate.

In order to examine the sustained antibacterial activity after exposure to physiological aqueous conditions, each composite was immersed in phosphate buffered saline (PBS, pH 7.4±0.1, WELGENE Inc, Gyeongsan, Korea) and kept under room temperature for 3 days. The surface of composite was rinsed with deionized water to remove released antibiotic moiety and dried at 60 °C for 5 h. Then the antibacterial activity

of composite was subjected to colony forming inhibition assay as described above.

RESULT AND DICUSSION

XRD

The crystal structure of pristine LDH and LL hybrid was investigated using X-ray diffraction patterns. Pristine LDH (Fig. 1A(a)) showed sharp characteristic peaks for hydrotalcite (JCPDS card No. 14-0191) as (003), (006), (012), (015) and (018) at 11.7°2θ, 23.5°2θ, 34.9°2θ, 41.7°2θ and 45.5°2θ, respectively (Oh et al., 2002; Wiyantoko et al., 2015). The d-value of pristine LDH was 0.76 nm corresponding to carbonate anions in the interlayer (Oh et al., 2002). Calcined LDH, i.e., LDO showed diffraction peaks at 35.2°2θ and 43.2°2θ, corresponding to (111) and (200) of periclase (JCPDS card No. 71-1176) (Fig. 1A(b)). The XRD patterns of LL hybrid (Fig. 1A(c)) exhibited (003) peak at 2.82°2θ, (009) peak at 8.46°2θ and (012) peak at 34.9°2θ. The (00l) peak shift to lower angle indicated that intercalation of larger molecules into LDH; the d-spacing of LDH increased from 0.76 nm to 3.13 nm upon LVX intercalation. The peak position preservation of (012) at 34.9°2θ indicated that there was no significant lattice deterioration upon LVX intercalation through reconstruction. Small peaks of (003) and (006) corresponding to d-spacing 0.76 nm were observed in the XRD pattern for LL, suggesting the potential existence of CO_3^{2-}. During reconstruction process, a part of LDO particles would undergo reconstruction with carbonate rather than with LVX.

The interlayer arrangement of LVX molecules in LDH was proposed in Fig. 1B based on Monte Carlo simulation starting from XRD data. The main interactions were electrostatic attraction between negative charge of LVX and positive LDH layer (Fig. 1B(c)) with approximately 2.1 Å of distance. Furthermore, it was found that the LVX molecules could interact to each other through pi-pi stacking with intermolecular distance ~4.2 Å (Fig. 1B(d)). Taking into account the theoretical values for molecular thickness of LVX (~7 Å), intermolecular distance (~4.2 Å), LVX-LDH distance (~2.1 Å) and layer thickness of LDH (~4.8 Å), the bilayer model of LVX molecules with parallel orientation was considered the most plausible interlayer structure (Fig. 1B(b)). The dual stabilization of LVX through electrostatic interaction and intermolecular pi-pi interaction is considered advantageous to immobilize drug moiety in LDH matrix.

The crystallinity along crystallographic c-axis directions was calculated by Scherrer's equation as

follows; $t = (0.9\lambda)/(B \cdot \cos\theta)$ where t: crystallite size, λ: X-ray wavelength, B: full-width-at-half-maximum, θ: Bragg angle) (Culity & Stock, 1978). The crystallite size along (003) plane reduced from 55.4 nm to 16.1 nm after hybridization. The reduced crystallite size was attributed to random stacking between LDH layers and organic moieties during reconstruction as previously reported (Kim et al., 2016).

FT-IR

The chemical property of LVX in the LL hybrid was confirmed through FT-IR spectra. The IR spectrum of pristine LDH (Fig. 2(a)) exhibited characteristic peaks of CO_3^{2-} stretching vibration and M-O vibration in hydroxide layers at 1370 and 800 cm^{-1}, respectively (Kim et al., 2011). The spectrum of LVX (Fig. 2(b)) showed characteristic peaks for carboxyl C=O at 1725 cm^{-1}, amines at 1294 cm^{-1} and C-F at 1087 cm^{-1} (Mouzam et al., 2011; Jalvandi et al., 2017; Nazar et al., 2017). After hybridization between pristine LDH and LVX through reconstruction, the amine and C-F stretching vibration of LVX and M-O vibration of hydroxyl layers were well preserved in the IR, suggesting the intact structure of drug inside LL hybrid (Fig. 2(c)). It was noteworthy that, after hybridization, the peak for carboxyl C=O disappeared and new peaks corresponding to antisymmetric and symmetric stretching vibration of COO^- occurred at 1582 cm^{-1} and 1400 cm^{-1} (Sultana et al., 2013; Al-Hussaini et al., 2018), respectively. The results revealed that carboxylic acid in LVX was deprotonated to be stabilized in LDH through electrostatic interaction. Through XRD patterns and IR spectra of pristine LDH and LL hybrid, it could be concluded that LVX was successfully intercalated into interlayer of LDH by reconstruction route.

Chemical formula

In order to determine chemical formula and LVX content of LL hybrid, ICP-OES and elemental analyses were utilized. The calculated Mg:Al ratio of metal hydroxide layer in LL hybrid was 0.69:0.31 (25.62% of C content and 4.9% for N content). As a result, the chemical formula of LL hybrid could be calculated as $[Mg_{0.69}Al_{0.31}(OH)_2]^{0.31+}[(OH)_{0.10}(LVX)_{0.13}(CO_3)_{0.04}]^{0.31-} \cdot 0.1H_2O$. Although the chemical formula contained three anionic species in the second parenthesis, it did not mean the co-intercalation of three species. As discussed in the XRD section, a part of LDO was considered to reconstruct to carbonate-LDH phase while most of LDO

transformed to LVX intercalated LDH. The LVX content in LL hybrid (loading capacity) was determined 41.7% from the chemical formula of LL hybrid, and this was fairly comparable with the theoretical loading. Considering the previous literature on drug-LDH hybrid (Oh et al., 2006; Kong et al., 2010), the LVX content in LL hybrid was sufficiently high to have drug efficacy and the existence of carbonate is not expected to have negative effect on its antibacterial performance.

SEM

The particle size and morphology of pristine LDH and LL hybrid were visualized using scanning electron microscopy. The SEM image of pristine LDH (Fig. 3(a)) showed the typical coin-like shape of LDH with average particle size 265 ± 42 nm. After hybridization with LVX by reconstruction, morphology of LDH changed to sand-rose shape which was formed by agglomeration of partially bent and thin layers (Fig. 3(b)) (Kang et al., 2015; Kim et al., 2018). This result well-matched with previous studies which demonstrated the formation of sand-rose morphology for organic-LDH hybrid resulting in partial delamination and increasing face to edge interaction during reconstruction process (Kim et al., 2018).

TEM

The cross-sectional TEM images (Fig. 4) showed the characteristic layered structure of LDH and visualized the expanded interlayer distance due to the intercalation of LVX. The interlayer distance of the LL corresponding to the periodic lattice fringe was confirmed to be 3.2 nm, and this value was in good agreement with the d_{003} value of LL hybrid (3.13 nm) in the XRD pattern (Fig. 1(b)). In addition, the energy dispersive spectroscopy (EDS) mapping for LL hybrid (Fig. 5) showed that the particles of the LL hybrid mainly composed of magnesium and aluminum elements forming LDH plate. Homogeneous distribution of nitrogen and fluorine was attributed to LVX moiety which was mixed with LDH lattice in nanometer scale. The results strongly supported that the LVX molecules were intercalated between LDH layer with high periodic arrangement.

SEM images of LVX and LL hybrid containing composite

Fig. 5 showed the SEM images of polyurethane (PU) after LVX or LL hybrid loading. LVX loaded PU composite (Fig. 5(a)) exhibited typical morphology of polymer material with smooth surface. On the other hand, SEM image of LL hybrid loaded PU showed particle-like morphology out of polymer matrix, which was attributed to the partially exposed LL hybrid. The inorganic part, LDH, in LL hybrid is expected to protect LVX from abrupt release from the polymer matrix.

LVX release study from LL hybrid

The LVX release in aqueous media (saline) from LL hybrid was tested in time-dependent manner. As shown in Fig. 7, the fractional release of LVX consisted of burst in initial stage (~5 min) followed by sustained release afterward, which corresponded to the typical release pattern of drug intercalated LDH (Gu et al., 2008; Senapati et al., 2016). In order to interpret the release kinetic, the profile was fitted to three representative models, first order, Elovich model and power function, respectively, as described in the Experimental section.

According to the literature, the three models hypothesizes the release condition as follows. First order describes the release behavior mainly mediated by dissolution (bin Hussein et al., 2002); Elovich model explains a release process through a bulk surface diffusion (Senapati et al., 2016); power function hypothesizes a release by diffusion from flat surfaces or ion exchange phenomena (Kang et al., 2015). The linear fitting results showed regression factor R^2 values of 0.786, 0.974, and 0.981 for first order, Elovich model, and power function, respectively, suggesting that the release of LVX was governed by a diffusion mediated by flat surface. In other words, the host LDH lattice played an important role in release control. Therefore, it was expected that the LL hybrid embedded in PU substrate release LVX in a restricted manner due to the action of flat LDH layer.

Antibacterial activity of LVX and LL hybrid

In order to compare antibacterial activity of LVX-PU and LL-PU composite, bacterial colony forming inhibition assay was carried out against Bacillus subtilis (B. sub). For the first step, the antibacterial activities of LVX and LL hybrid were compared. As a preliminary study, both samples with 0.5, 1.0 and 2.5 ppm of drug

concentration was treated to the bacteria and the concentration point 1.0 ppm was selected as the minimal concentration to show 100% antibacterial activity. It was noteworthy that LL hybrid, which contained drug moiety inside its gallery space, showed the same antibacterial activity with LVX at drug concentration of 1.0 ppm (Fig. 8). According to the previous study (Al-Hussaini et al., 2018b), LVX and LVX-intercalated LDH exhibited antibiotic inhibition zone in paper disc assay above 5 ppm concentration. The literature showed relative lower antibacterial effect of LVX-LDH than LVX alone. Although the previous data of paper disc assay cannot be directly compared with current colony forming assay, the current LL hybrid could be considered to contain comparable antibacterial effect with LVX alone at fairly low concentration. The effectiveness of LL hybrid in antibacterial effect could be ascribed by the concentrated drug release at the interface between LL particle and microbe. Different from LVX solution where the LVX concentration was even everywhere, the LL hybrid had heterogeneous concentration distribution — the LVX moiety was converged in LL particles. Thus, LL particle could exhibit high bactericidal effect if it encountered microbes.

Then, the antibacterial activity of LVX-PU and LL-PU composite containing 5.0 mg LVX per 1.0 g composite was evaluated (Fig. 9). As prepared LVX-PU and LL-PU composite showed 100% antibacterial activity against B. sub as expected from the efficacy of material itself. This could be straightforwardly expected by the high antibacterial effect of both LVX and LL (Fig. 8). The microbes attached on the surface of films would be readily influenced by the drug moiety which was exposed at the composite surface or partially released from the inside of composite. This kind of ready antibacterial action could diminish when the material is continuously placed in aqueous condition, for instance, in implantable device or liquid flowing medial tube. In order to control release of antibiotics in solid substrate, various methods have been suggested. Vasilev et al. sandwiched LVX moiety by plasma polymerized layers on a solid substrate to control release depending on layer-thickness (2011). They showed that ~50% of drug release could be suppressed within 30 h under PBS condition. In another approach, LVX was first encapsulated by β-cyclodextrin which was further grafted to polypropylene-based medical mesh which showed sustained antibacterial efficacy until 7 days (Sanbhal et al., 2018). Antibacterial moiety could be directly conjugated with polymers for dental implant application (Zhang et al., 2019), where sustained release of drug moiety was observed for 25 days in PBS condition. Similar to the previous works, current system was designed to retard release of embedded drug moiety. The immersion of both composites in PBS for 3 days dramatically changed the antibacterial efficacy of materials. The antibacterial activity of LVX-PU composite dropped down to 0% upon PBS immersion; on the other hand, the antibacterial

activity of LL-PU composite fairly remained showing ~34% of colony forming inhibition. From the antibacterial activity of LVX-PU and LL-PU composite before and after immersion in PBS for 3 days, it was confirmed that LL-PU composite have sustained antibacterial activity compared with LVX-PU in physiological condition. Water soluble drug like LVX can be easily washed off from the polymer substrate when it is placed under aqueous condition. Ragel et al. prepared composite among bioactive glass, biopolymer and water soluble drug, gentamicin (2000). Due to the highly water-soluble property, 80% of drug was readily released from the composite within 1 day in physiological solution. Current LVX-PU composite would undergo similar process of fast release. However, as expected in the release section, the release of LVX in LL hybrid was controlled by the flat surface of LDH layers, and thus it would take more steps of LVX molecules to escape from the composite. In this way, the LL-PU composite is considered to suppress drug release and to prolong antibacterial effect under aqueous condition.

CONCLUSION

Hybrid between LVX and LDH by reconstruction was prepared to immobilize antibiotic in composite and to expect sustained antibacterial activity of polymer containing hybrid. The XRD patterns and FT-IR spectra of pristine LDH and LL hybrid exhibited that LVX was successfully intercalated into interlayer of LDH by reconstruction route. According to the ICP-OES and elemental analysis, the hybrid was found to have 41.7% of LVX loading capacity. The SEM images of pristine LDH and LL hybrid showed that coin-like shape of pristine LDH with 265 ± 42 nm particle size was changed to sand-rose shape with heterogeneous particle size which was typical pattern found in reconstruction. From the cross-sectional TEM analysis with EDS mapping, the interlayer distance of LL hybrid was determined to match with d-value from XRD patterns as ~ 3.2 nm and the composition of metal layer (Mg and Al) and LVX (N and F) was well distributed throughout LL hybrid. Both LVX-PU and LL-PU composite showed 100% antibacterial activity against B. subtilis as prepared. After immersion in PBS for 3 days, however, the antibacterial activity of LVX-PU composite dropped down to 0%, while LL-PU composite maintained ~34% antibacterial activity.

ACKNOWLEDGMENT

This work was supported by the Dongguk University Research Fund of 2019.

Compliance with Ethical Standards

Conflict of Interest: The authors declare that they have no conflict of interest

Reference

Al-Hussaini, S., Al-Ghanimi, A. & Kadhim, H.J.S.J.M.R. (2018) Preparation of nanohybrid antibiotic from levofloxacin and determination its inhibitory efficacy against staphylococcus aureus isolated from diabetic foot ulcer. *Scientific Journal of Medical Research*, **2**, 29–35.

bin Hussein, M.Z., Zainal, Z., Yahaya, A.H. & Foo, D.W.V. (2002) Controlled release of a plant growth regulator, α-naphthaleneacetate from the lamella of zn–al-layered double hydroxide nanocomposite. *Journal of Controlled Release*, **82**, 417–427.

Cavani, F., Trifirò, F. & Vaccari, A. (1991) Hydrotalcite-type anionic clays: Preparation, properties and applications. *Catalysis Today*, **11**, 173–301.

Choy, J.-H., Kwak, S.-Y., Jeong, Y.-J. & Park, J.-S. (2000) Inorganic layered double hydroxides as nonviral vectors. *Angewandte Chemie International Edition*, **39**, 4041–4045.

Choy, J.-H., Kwak, S.-Y., Park, J.-S., Jeong, Y.-J. & Portier, J. (1999) Intercalative nanohybrids of nucleoside monophosphates and DNA in layered metal hydroxide. *Journal of the American Chemical Society*, **121**, 1399–1400.

Conlon, B.P., Nakayasu, E.S., Fleck, L.E., LaFleur, M.D., Isabella, V.M., Coleman, K., Leonard, S.N., Smith, R.D., Adkins, J.N. & Lewis, K. (2013) Activated clpp kills persisters and eradicates a chronic biofilm infection. *Nature*, **503**, 365–370.

Culity, B. & Stock, S.J.E.-W.P.C.I., USA. (1978) Elements of x-ray diffraction 2 nd ed.

Garcez, A.S., Ribeiro, M.S., Tegos, G.P., Núñez, S.C., Jorge, A.O.C. & Hamblin, M.R. (2007) Antimicrobial photodynamic therapy combined with conventional endodontic treatment to eliminate root canal biofilm infection. *Lasers in Surgery and Medicine*, **39**, 59–66.

Geuli, O., Metoki, N., Zada, T., Reches, M., Eliaz, N. & Mandler, D. (2017) Synthesis, coating, and drug-release of hydroxyapatite nanoparticles loaded with antibiotics. *Journal of Materials Chemistry B*, **5**, 7819–7830.

Gu, Z., Thomas, A.C., Xu, Z.P., Campbell, J.H. & Lu, G.Q. (2008) In vitro sustained release of lmwh from mgal-layered double hydroxide nanohybrids. *Chemistry of Materials*, **20**, 3715–3722.

Hoffman, L.R., D'Argenio, D.A., MacCoss, M.J., Zhang, Z., Jones, R.A. & Miller, S.I. (2005) Aminoglycoside antibiotics induce bacterial biofilm formation. *Nature*, **436**, 1171–1175.

Hong, Y., Xi, Y., Zhang, J., Wang, D., Zhang, H., Yan, N., He, S. & Du, J. (2018) Polymersome–hydrogel composites with combined quick and long-term antibacterial activities. *Journal of Materials Chemistry B*, **6**, 6311–6321.

Hu, J., Quan, Y., Lai, Y., Zheng, Z., Hu, Z., Wang, X., Dai, T., Zhang, Q. & Cheng, Y. (2017) A smart aminoglycoside hydrogel with tunable gel degradation, on-demand drug release, and high antibacterial activity. *Journal of Controlled Release*, **247**, 145–152.

Jalvandi, J., White, M., Gao, Y., Truong, Y.B., Padhye, R. & Kyratzis, I.L. (2017) Polyvinyl alcohol composite nanofibres containing conjugated levofloxacin-chitosan for controlled drug release. *Materials Science and Engineering: C*, **73**, 440–446.

Kang, H., Kim, H.-J., Yang, J.-H., Kim, T.-H., Choi, G., Paek, S.-M., Choi, A.-J., Choy, J.-H. & Oh, J.-M. (2015) Intracrystalline structure and release pattern of ferulic acid intercalated into layered double hydroxide through various synthesis routes. *Applied Clay Science*, **112–113**, 32–39.

Khodaverdi, E., Soleimani, H.A., Mohammadpour, F. & Hadizadeh, F. (2016) Synthetic

zeolites as controlled-release delivery systems for anti-inflammatory drugs. *Chemical Biology & Drug Design*, **87**, 849–857.

Kim, H.-J., Kim, T.-H., Kim, H.-M., Hong, I.-K., Kim, E.-J., Choi, A.-J., Choi, H.-J. & Oh, J.-M. (2016) Nano-biohybrids of engineered nanoclays and natural extract for antibacterial agents. *Applied Clay Science*, **134**, 19–25.

Kim, H.-J., Lee, G.J., Choi, A.-J., Kim, T.-H., Kim, T.-i. & Oh, J.-M. (2018) Layered double hydroxide nanomaterials encapsulating angelica gigas nakai extract for potential anticancer nanomedicine. *Frontiers in Pharmacology*, **9**. 723

Kim, K.-M., Park, C.-B., Choi, A-J., Choi, H.-J. & Oh, J.-M. (2011) Selective DNA adsorption on layered double hydroxide nanoparticles. *Bulletin of the Korean Chemical Society*, **32**, 2217–2221.

Kim, T.-H., Hong, I.T. & Oh, J.-M. (2018) Size- and surface charge-controlled layered double hydroxides for efficient algal flocculation. *Environmental Science: Nano*, **5**, 183–190.

Kim, T.-H., Kim, H.-J., Choi, A.-J., Choi, H.-J. & Oh, J.-M. (2016) Hybridization between natural extract of angelica gigas nakai and inorganic nanomaterial of layered double hydroxide via reconstruction reaction. *Journal of Nanoscience and Nanotechnology*, **16**, 1138–1145.

Kong, X., Jin, L., Wei, M. & Duan, X. (2010) Antioxidant drugs intercalated into layered double hydroxide: Structure and in vitro release. *Applied Clay Science*, **49**, 324–329.

Latifi, L., Sohrabnezhad, S. & Hadavi, M. (2017) Mesoporous silica as a support for poorly soluble drug: Influence of ph and amino group on the drug release. *Microporous and Mesoporous Materials*, **250**, 148–157.

Lucke, M., Schmidmaier, G., Sadoni, S., Wildemann, B., Schiller, R., Haas, N.P. & Raschke, M. (2003) Gentamicin coating of metallic implants reduces implant-related osteomyelitis in rats. *Bone*, **32**, 521–531.

Mouzam, M.I., Dehghan, M.H.G., Asif, S., Sahuji, T. & Chudiwal, P. (2011) Preparation of a novel floating ring capsule-type dosage form for stomach specific delivery. *Saudi Pharmaceutical Journal*, **19**, 85–93.

Nazar, M.F., Saleem, M.A., Bajwa, S.N., Yameen, B., Ashfaq, M., Zafar, M.N. & Zubair, M. (2017) Encapsulation of antibiotic levofloxacin in biocompatible microemulsion formulation: Insights from microstructure analysis. *The Journal of Physical Chemistry B*, **121**, 437–443.

Oh, J.-M., Hwang, S.-H. & Choy, J.-H. (2002) The effect of synthetic conditions on tailoring the size of hydrotalcite particles. *Solid State Ionics*, **151**, 285–291.

Oh, J.-M., Park, M., Kim, S.-T., Jung, J.-Y., Kang, Y.-G. & Choy, J.-H. (2006) Efficient delivery of anticancer drug mtx through mtx-ldh nanohybrid system. *Journal of Physics and Chemistry of Solids*, **67**, 1024–1027.

Olanoff, L.S., Anderson, J.M. & Jones, R.D. (1979) Sustained release of gentamicin from prosthetic heart valves. *ASAIO Journal*, **25**, 334–338.

Patel, D.K., Biswas, A. & Maiti, P. (2016) 6 - nanoparticle-induced phenomena in polyurethanes. Pp. 171-194. In S.L. Cooper, and J. Guan, Eds. *Advances in polyurethane biomaterials*,Woodhead Publishing.

Pinto, F.C.H., Silva-Cunha, A., Pianetti, G.A., Ayres, E., Oréfice, R.L. & Da Silva, G.R. (2011) Montmorillonite clay-based polyurethane nanocomposite as local triamcinolone acetonide delivery system. *Journal of Nanomaterials*, **2011**, 1–11.

Ragel, C.V. & Vallet–Regí, M. (2000) In vitro bioactivity and gentamicin release from glass–polymer–antibiotic composites. *Journal of Biomedical Materials Research*, **51**, 424–

429.
Rives, V. (2001) *Layered double hydroxides: Present and future*. Nova Publishers.
Saha, K., Butola, B.S. & Joshi, M. (2014) Drug release behavior of polyurethane/clay nanocomposite: Film vs. Nanofibrous web. *Journal of Applied Polymer Science*, **131**, 40824.
Sanbhal, N., Saitaer, X., Li, Y., Mao, Y., Zou, T., Sun, G. & Wang, L.J.P. (2018) Controlled levofloxacin release and antibacterial properties of β-cyclodextrins-grafted polypropylene mesh devices for hernia repair. **10**, 493.
Senapati, S., Thakur, R., Verma, S.P., Duggal, S., Mishra, D.P., Das, P., Shripathi, T., Kumar, M., Rana, D. & Maiti, P. (2016) Layered double hydroxides as effective carrier for anticancer drugs and tailoring of release rate through interlayer anions. *Journal of Controlled Release*, **224**, 186–198.
Sultana, N., Arayne, M.S., Rizvi, S.B.S., Haroon, U. & Mesaik, M.A. (2013) Synthesis, spectroscopic, and biological evaluation of some levofloxacin metal complexes. *Medicinal Chemistry Research*, **22**, 1371–1377.
Traba, C. & Liang, J.F. (2015) Bacteria responsive antibacterial surfaces for indwelling device infections. *Journal of Controlled Release*, **198**, 18–25.
Vasilev, K., Poulter, N., Martinek, P. & Griesser, H.J. (2011) Controlled release of levofloxacin sandwiched between two plasma polymerized layers on a solid carrier. *ACS Applied Materials & Interfaces*, **3**, 4831–4836.
Wang, C.-H., Hou, G.-G., Du, Z.-Z., Cong, W., Sun, J.-F., Xu, Y.-Y. & Liu, W.-S. (2016) Synthesis, characterization and antibacterial properties of polyurethane material functionalized with quaternary ammonium salt. *Polymer Journal*, **48**, 259–265.
Wiyantoko, B., Kurniawati, P., Purbaningtias, T.E. & Fatimah, I. (2015) Synthesis and characterization of hydrotalcite at different mg/al molar ratios. *Procedia Chemistry*, **17**, 21–26.
Zhang, R., Jones, M.M., Moussa, H., Keskar, M., Huo, N., Zhang, Z., Visser, M.B., Sabatini, C., Swihart, M.T. & Cheng, C. (2019) Polymer–antibiotic conjugates as antibacterial additives in dental resins. *Biomaterials Science*, **7**, 287–295.

Reference

Al-Hussaini, S., Al-Ghanimi, A. & Kadhim, H.J.S.J.M.R. (2018a) Preparation of nanohybrid antibiotic from levofloxacin and determination its inhibitory efficacy against staphylococcus aureus isolated from diabetic foot ulcer. *Scientific Journal of Medical Research*, **2**, 29-35.

-. (2018b) Preparation of nanohybrid antibiotic from levofloxacin and determination its inhibitory efficacy against staphylococcus aureus isolated from diabetic foot ulcer. **2**, 29-35.

bin Hussein, M.Z., Zainal, Z., Yahaya, A.H. & Foo, D.W.V. (2002) Controlled release of a plant growth regulator, α-naphthaleneacetate from the lamella of zn–al-layered double hydroxide nanocomposite. *Journal of Controlled Release*, **82**, 417-427.

Cavani, F., Trifirò, F. & Vaccari, A. (1991) Hydrotalcite-type anionic clays: Preparation, properties and applications. *Catalysis Today*, **11**, 173-301.

Choy, J.-H., Kwak, S.-Y., Jeong, Y.-J. & Park, J.-S. (2000) Inorganic layered double hydroxides as nonviral vectors. *Angewandte Chemie International Edition*, **39**, 4041-4045.

Choy, J.-H., Kwak, S.-Y., Park, J.-S., Jeong, Y.-J. & Portier, J. (1999) Intercalative nanohybrids of nucleoside monophosphates and DNA in layered metal hydroxide. *Journal of the American Chemical Society*, **121**, 1399-1400.

Conlon, B.P., Nakayasu, E.S., Fleck, L.E., LaFleur, M.D., Isabella, V.M., Coleman, K., Leonard, S.N., Smith, R.D., Adkins, J.N. & Lewis, K. (2013) Activated clpp kills persisters and eradicates a chronic biofilm infection. *Nature*, **503**, 365-370.

Culity, B. & Stock, S.J.E.-W.P.C.I., USA. (1978) Elements of x-ray diffraction 2 nd ed.

Garcez, A.S., Ribeiro, M.S., Tegos, G.P., Núñez, S.C., Jorge, A.O.C. & Hamblin, M.R. (2007) Antimicrobial photodynamic therapy combined with conventional endodontic treatment to eliminate root canal biofilm infection. *Lasers in Surgery and Medicine*, **39**, 59-66.

Geuli, O., Metoki, N., Zada, T., Reches, M., Eliaz, N. & Mandler, D. (2017) Synthesis, coating, and drug-release of hydroxyapatite nanoparticles loaded with antibiotics. *Journal of Materials Chemistry B*, **5**, 7819-7830.

Gu, Z., Thomas, A.C., Xu, Z.P., Campbell, J.H. & Lu, G.Q. (2008) In vitro sustained release of lmwh from mgal-layered double hydroxide nanohybrids. *Chemistry of Materials*, **20**, 3715-3722.

Hoffman, L.R., D'Argenio, D.A., MacCoss, M.J., Zhang, Z., Jones, R.A. & Miller, S.I. (2005) Aminoglycoside antibiotics induce bacterial biofilm formation. *Nature*, **436**, 1171-1175.

Hong, Y., Xi, Y., Zhang, J., Wang, D., Zhang, H., Yan, N., He, S. & Du, J. (2018) Polymersome–hydrogel composites with combined quick and long-term antibacterial activities. *Journal of Materials Chemistry B*, **6**, 6311-6321.

Hu, J., Quan, Y., Lai, Y., Zheng, Z., Hu, Z., Wang, X., Dai, T., Zhang, Q. & Cheng, Y. (2017) A smart aminoglycoside hydrogel with tunable gel degradation, on-demand drug release, and high antibacterial activity. *Journal of Controlled Release*, **247**, 145-152.

Jalvandi, J., White, M., Gao, Y., Truong, Y.B., Padhye, R. & Kyratzis, I.L. (2017) Polyvinyl alcohol composite nanofibres containing conjugated levofloxacin-chitosan for controlled drug release. *Materials Science and Engineering: C*, **73**, 440-446.

Kang, H., Kim, H.-J., Yang, J.-H., Kim, T.-H., Choi, G., Paek, S.-M., Choi, A.-J., Choy, J.-H. & Oh, J.-M. (2015) Intracrystalline structure and release pattern of ferulic acid intercalated into layered double hydroxide through various synthesis routes. *Applied Clay Science*, **112-113**, 32-39.

Khodaverdi, E., Soleimani, H.A., Mohammadpour, F. & Hadizadeh, F. (2016) Synthetic zeolites as controlled-release delivery systems for anti-inflammatory drugs. *Chemical Biology & Drug Design*, **87**, 849-857.

Kim, H.-J., Kim, T.-H., Kim, H.-M., Hong, I.-K., Kim, E.-J., Choi, A.-J., Choi, H.-J. & Oh, J.-M. (2016a) Nano-biohybrids of engineered nanoclays and natural extract for antibacterial agents. *Applied Clay Science*, **134**, 19-25.

Kim, H.-J., Lee, G.J., Choi, A.-J., Kim, T.-H., Kim, T.-i. & Oh, J.-M. (2018a) Layered double hydroxide nanomaterials encapsulating angelica gigas nakai extract for potential anticancer nanomedicine. *Frontiers in Pharmacology*, **9**.

Kim, K.-M., Park, C.-B., 최애진, 최진호 & 오제민. (2011) *Bulletin of the Korean Chemical Society*, **32**, 2217-2221.

Kim, T.-H., Hong, I.T. & Oh, J.-M. (2018b) Size- and surface charge-controlled layered double hydroxides for efficient algal flocculation. *Environmental Science: Nano*, **5**, 183-190.

Kim, T.-H., Kim, H.-J., Choi, A.-J., Choi, H.-J. & Oh, J.-M. (2016b) Hybridization between natural extract of angelica gigas nakai and inorganic nanomaterial of layered double hydroxide via reconstruction reaction. *Journal of Nanoscience and Nanotechnology*, **16**, 1138-1145.

Kong, X., Jin, L., Wei, M. & Duan, X. (2010) Antioxidant drugs intercalated into layered double hydroxide: Structure and in vitro release. *Applied Clay Science*, **49**, 324-329.

Latifi, L., Sohrabnezhad, S. & Hadavi, M. (2017) Mesoporous silica as a support for poorly soluble drug: Influence of ph and amino group on the drug release. *Microporous and Mesoporous Materials*, **250**, 148-157.

Lucke, M., Schmidmaier, G., Sadoni, S., Wildemann, B., Schiller, R., Haas, N.P. & Raschke, M. (2003) Gentamicin coating of metallic implants reduces implant-related osteomyelitis in rats. *Bone*, **32**, 521-531.

Mouzam, M.I., Dehghan, M.H.G., Asif, S., Sahuji, T. & Chudiwal, P. (2011) Preparation of a novel floating ring capsule-type dosage form for stomach specific delivery. *Saudi Pharmaceutical Journal*, **19**, 85-93.

Nazar, M.F., Saleem, M.A., Bajwa, S.N., Yameen, B., Ashfaq, M., Zafar, M.N. & Zubair, M. (2017) Encapsulation of antibiotic levofloxacin in biocompatible microemulsion formulation: Insights from microstructure analysis. *The Journal of Physical Chemistry B*, **121**, 437-443.

Oh, J.-M., Hwang, S.-H. & Choy, J.-H. (2002) The effect of synthetic conditions on tailoring the size of hydrotalcite particles. *Solid State Ionics*, **151**, 285-291.

Oh, J.-M., Park, M., Kim, S.-T., Jung, J.-Y., Kang, Y.-G. & Choy, J.-H. (2006) Efficient delivery of anticancer drug mtx through mtx-ldh nanohybrid system. *Journal of Physics and Chemistry of Solids*, **67**, 1024-1027.

Olanoff, L.S., Anderson, J.M. & Jones, R.D. (1979) Sustained release of gentamicin from prosthetic heart valves. *ASAIO Journal*, **25**.

Patel, D.K., Biswas, A. & Maiti, P. (2016) 6 - nanoparticle-induced phenomena in polyurethanes. Pp. 171-194. In S.L. Cooper, and J. Guan, Eds. *Advances in polyurethane biomaterials*,Woodhead Publishing.

Pinto, F.C.H., Silva-Cunha, A., Pianetti, G.A., Ayres, E., Oréfice, R.L. & Da Silva, G.R. (2011) Montmorillonite clay-based polyurethane nanocomposite as local triamcinolone acetonide delivery system. *Journal of Nanomaterials*, **2011**, 1-11.

Ragel, C.V. & Vallet–Regí, M. (2000) In vitro bioactivity and gentamicin release from glass–polymer–antibiotic composites. *Journal of Biomedical Materials Research*, **51**, 424-429.

Rives, V. (2001) *Layered double hydroxides: Present and future*. Nova Publishers.

Saha, K., Butola, B.S. & Joshi, M. (2014) Drug release behavior of polyurethane/clay nanocomposite: Film vs. Nanofibrous web. *Journal of Applied Polymer Science*, **131**.

Sanbhal, N., Saitaer, X., Li, Y., Mao, Y., Zou, T., Sun, G. & Wang, L.J.P. (2018) Controlled levofloxacin release and antibacterial properties of β-cyclodextrins-grafted polypropylene mesh devices for hernia repair. **10**, 493.

Senapati, S., Thakur, R., Verma, S.P., Duggal, S., Mishra, D.P., Das, P., Shripathi, T., Kumar, M., Rana, D. & Maiti, P. (2016) Layered double hydroxides as effective carrier for anticancer drugs and tailoring of release rate through interlayer anions. *Journal of Controlled Release*, **224**, 186-198.

Sultana, N., Arayne, M.S., Rizvi, S.B.S., Haroon, U. & Mesaik, M.A. (2013) Synthesis, spectroscopic, and biological evaluation of some levofloxacin metal complexes. *Medicinal Chemistry Research*, **22**, 1371-1377.

Traba, C. & Liang, J.F. (2015) Bacteria responsive antibacterial surfaces for indwelling device infections. *Journal of Controlled Release*, **198**, 18-25.

Vasilev, K., Poulter, N., Martinek, P. & Griesser, H.J. (2011) Controlled release of levofloxacin sandwiched between two plasma polymerized layers on a solid carrier. *ACS Applied Materials & Interfaces*, **3**, 4831-4836.

Wang, C.-H., Hou, G.-G., Du, Z.-Z., Cong, W., Sun, J.-F., Xu, Y.-Y. & Liu, W.-S. (2016) Synthesis, characterization and antibacterial properties of polyurethane material functionalized with quaternary ammonium salt. *Polymer Journal*, **48**, 259-265.

Wiyantoko, B., Kurniawati, P., Purbaningtias, T.E. & Fatimah, I. (2015) Synthesis and characterization of hydrotalcite at different mg/al molar ratios. *Procedia Chemistry*, **17**, 21-26.

Zhang, R., Jones, M.M., Moussa, H., Keskar, M., Huo, N., Zhang, Z., Visser, M.B., Sabatini, C., Swihart, M.T. & Cheng, C. (2019) Polymer–antibiotic conjugates as antibacterial additives in dental resins. *Biomaterials Science*, **7**, 287-295.

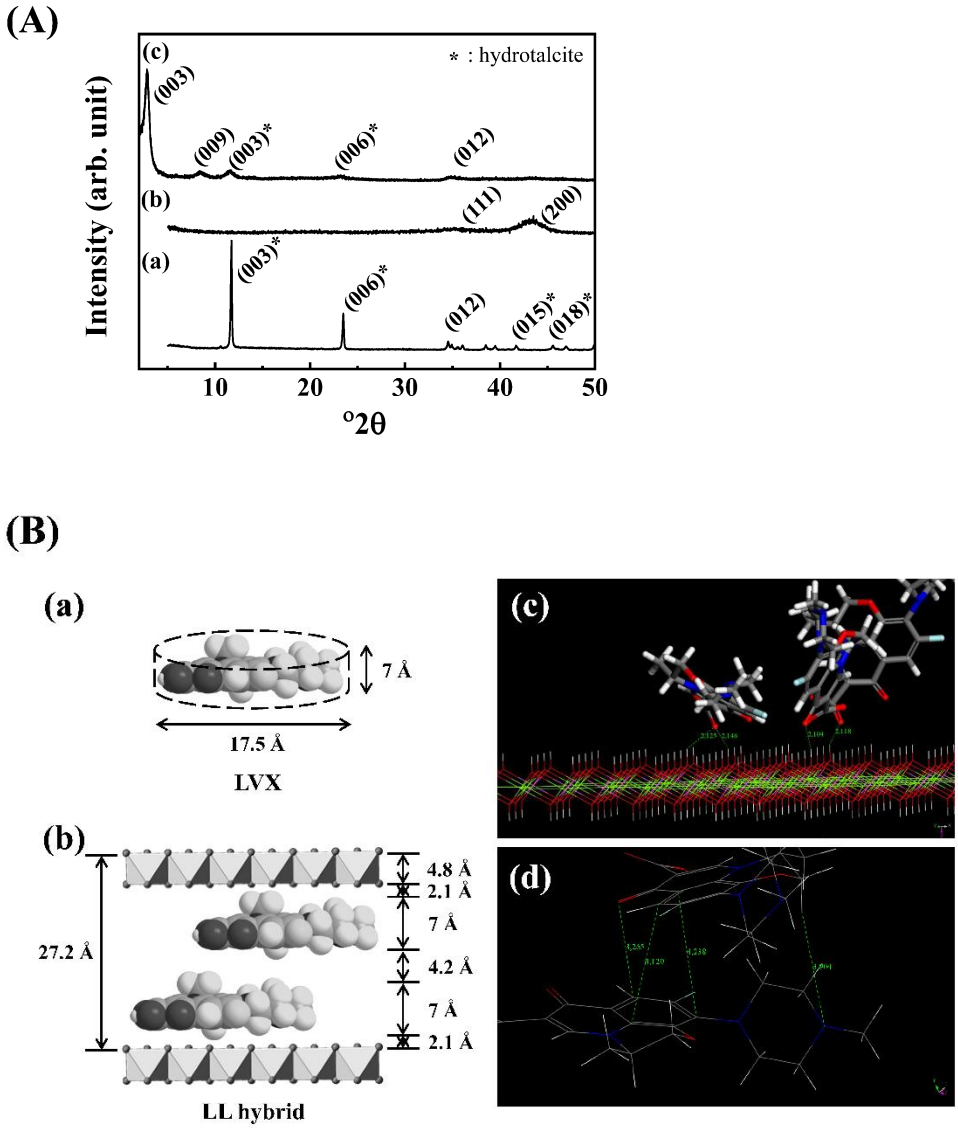

Fig. 1. (A) X-ray diffraction patterns for (a) pristine LDH (b) LDO and (c) LL hybrids. (B) (a) Schematic dimensions of LVX, (b) proposed interlayer arrangement of LL hybrid, (c) Main interactions between LVX and LDH layer extracted from Monte Carlo simulations, and (d) Illustration of the pi-stacking effect between LVX in the interlayer space, extracted from Monte Carlo simulations.

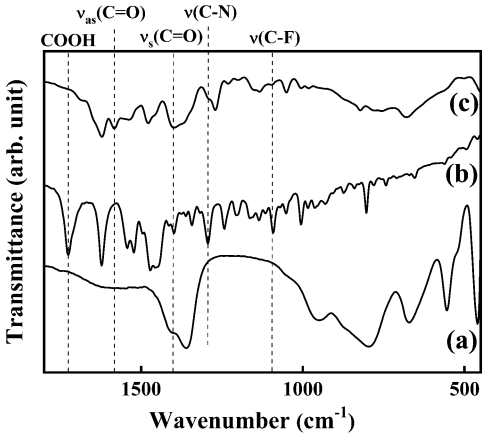

Fig. 2. Fourier transform infrared spectra for (a) LDH, (b) LVX and (c) LL.

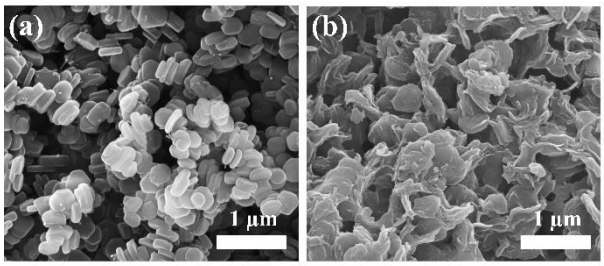

Fig. 3. Scanning electron microscope images for (a) pristine LDH and (b) LL hybrid.

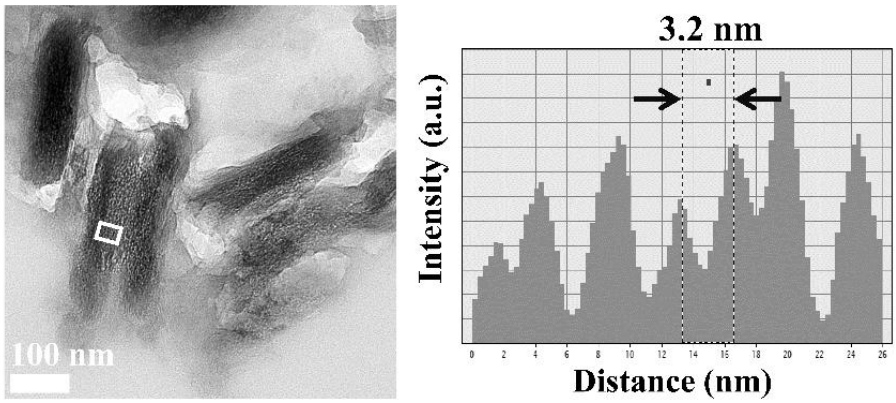

Fig. 4. Cross-sectional TEM image with histogram along (00l) direction for LL hybrid.

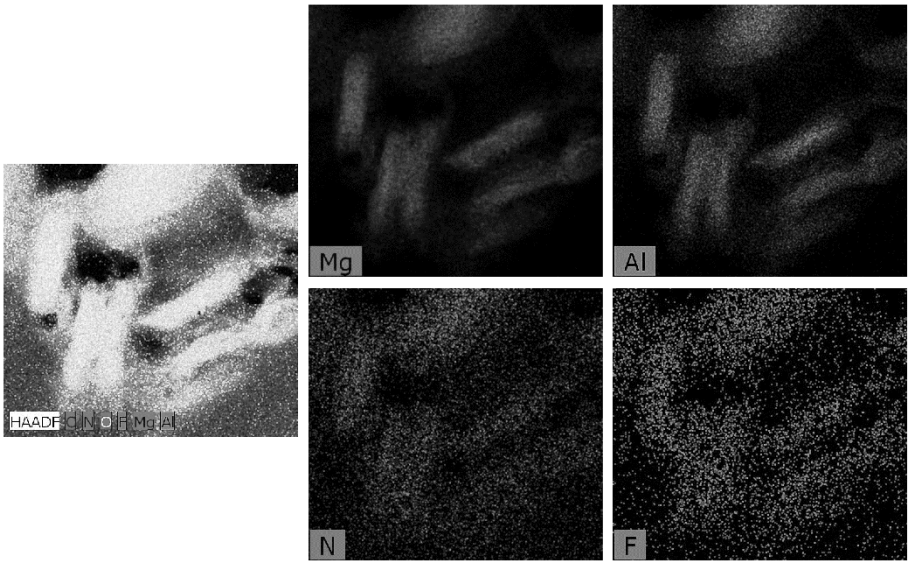

Fig. 5. Energy dispersive spectroscopy (EDS) mapping for LL hybrid.

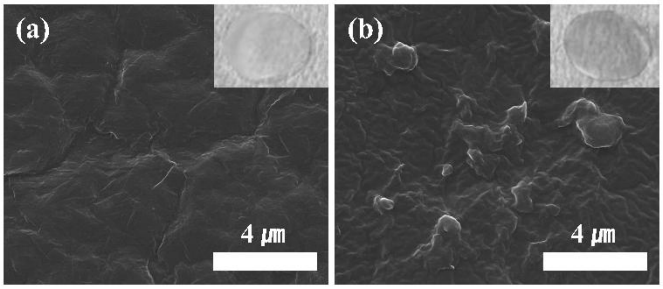

Fig. 6. Scanning electron microscopic images for surface of (a) LVX-PU and (b) LL-PU composite. Inset was photograph of each sample.

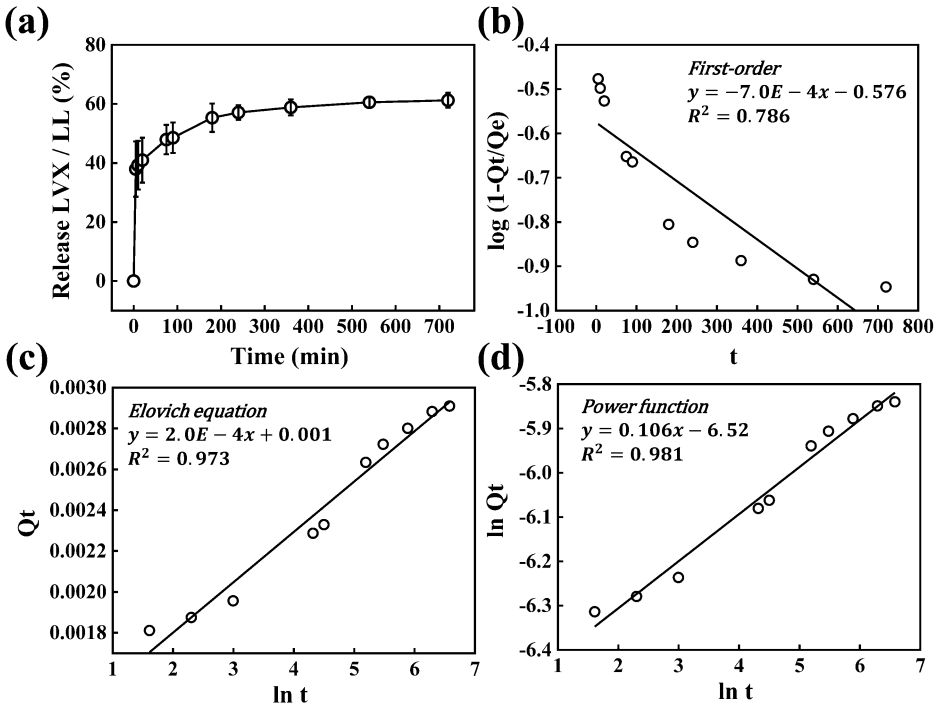

Fig. 7. Time dependent LVX release from LL hybrid in saline media.

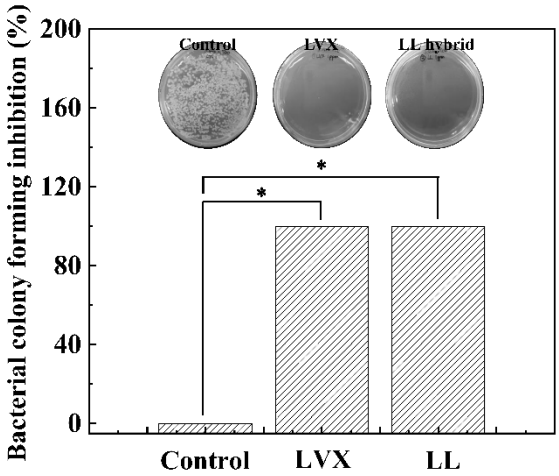

Fig. 8. Bacterial colony forming (%) of LVX solution and LL hybrid suspension on *Bacillus subtilis*. Asterisk stands for the statistical equivalence and difference with confidence intervals of 100% calculated by Student's *t*-test.

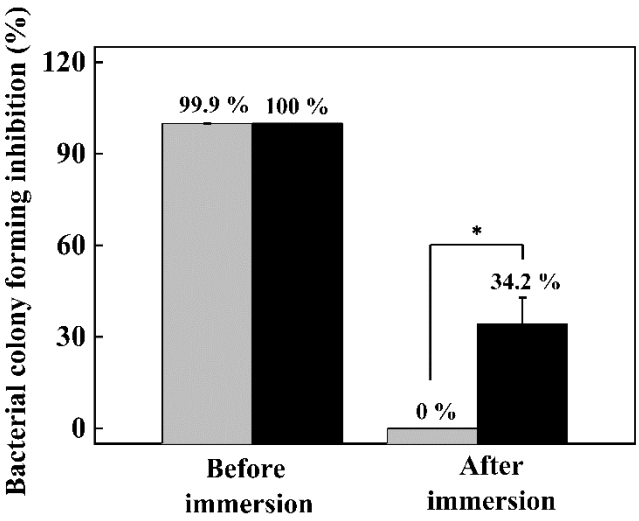

Fig. 9. Bacterial colony forming inhibition (%) of LVX-PU (gray bar) and LL-PU (black bar) composite against *Bacillus subtilis*. Either composite was immersed into phosphate buffered saline simulating biological condition. Single asterisk stands for statistical difference in 99.5% of confidence interval.